

1 **Testing the validity of regional detail in global analyses of Sea**  
2 **surface temperature — the case of Chinese coastal waters**

3 Yan Li<sup>1\*</sup>, Hans von Storch<sup>2,3</sup>, Qingyuan Wang<sup>4</sup>, Qingliang Zhou<sup>5</sup>, Shengquan Tang<sup>2,3</sup>

4 <sup>1</sup>National Marine Data and Information Service, Tianjin, People's Republic of China

5 <sup>2</sup>Institut für Küstenforschung, Helmholtz Zentrum Geesthacht, Germany

6 <sup>3</sup>Ocean University of China, Qingdao, People's Republic of China

7 <sup>4</sup>Tianjin Meteorological Observatory, Tianjin, People's Republic of China

8 <sup>5</sup>Chinese Meteorological Administration, Beijing, People's Republic of China

9

10 **Abstract.** We have designed a method for testing the quality of multidecadal analyses of SST  
11 in regional seas by using a set of high-quality local SST observations. In recognizing that  
12 local data may reflect local effects, we focus on dominant EOFs of the local data and of the  
13 localized data of the gridded SST analyses. We examine the patterns, variability as well as  
14 trends of the principal components. This method is applied to examine three different SST  
15 analyses, i.e., HadISST1, ERSST and COBE SST. They have been assessed using a newly  
16 constructed high-quality data set of SST at 26 coastal stations along the Chinese coast in  
17 1960–2015 which underwent careful examination with respect to quality, and a number of  
18 corrections of inhomogeneities. The three gridded analyses perform by and large well from  
19 1960 to 2015, in particular since 1980. However, for the pre-satellite period, prior to 1980s,  
20 the analyses differ among each other and show some inconsistencies with the local data, such  
21 as artificial break points, periods of bias and differences in trends. We conclude that gridded  
22 SST-analyses need improvement in the pre-satellite period (prior to 1980s), by re-examining  
23 in detail archives of local quality-controlled SST data in many data-sparse regions of the  
24 world.

25

---

\* Corresponding author. E-mail address: ly\_nmdis@163.com

## 26 **1. Introduction**

27 Sea surface temperature (SST) is a key parameter for climate change assessments. It is  
28 significantly associated with many atmospheric and oceanographic modes, such as Pacific  
29 Decadal Oscillation (PDO), El Niño/South Oscillation (ENSO), Indian Ocean Dipole (IOD),  
30 etc. (Saji et al., 1999, Mantua and Hare, 2002, Yeh and Kim, 2010). Long-term historical SST  
31 data sets have been extensively used as a source of information on global and regional SST  
32 trends and variability (Belkin, 2009; Wu et al., 2012; Boehme et al.2014; Hirahara et al.2014;  
33 Stramska and Bialogrodzka, 2015). However, historical SST datasets have large uncertainties  
34 in long-term trend patterns in some regions. For example, observed SST changes in the  
35 tropical Pacific are still controversial, depending on the choice of the dataset and study period  
36 (Bunge & Clarke 2009). Vecchiga et al. (2008) indicated that the equatorial zonal SST  
37 gradient in the Pacific has intensified in Hadley Centre Sea Ice and Sea Surface Temperature  
38 (HadISST) but weakened in Extended Reconstructed SST (ERSST) from the nineteenth to  
39 twentieth centuries. Scientists utilized several different datasets, including the reconstructed  
40 and un-interpolated datasets, to study the SST variability in tropical areas and the China Seas  
41 (Xie et al., 2010; Liu and Zhang 2013, Tokinaga et al., 2012). They found that there were  
42 large uncertainties in estimate of SST warming patterns using different SST datasets. Thus, it  
43 is also necessary for comparing different SST products over the regional areas in detail.

44 Coastal marine ecosystems yield nearly half of the earth's total ecosystem goods and services  
45 (Costanza, 1997). A study of SST changes in the world ocean with large marine ecosystems  
46 revealed that the Subarctic Gyre, European Seas, and East Asian Seas warmed at rates 2–4  
47 times the global mean rate (Belkin 2009). Recently, Lima and Wethey 2012 using a SST  
48 dataset with higher spatial-temporal resolution detected that during the last three decades ~  
49 71.6% of the world coastal locations have experienced a warming trend of  $0.25 \pm 0.13$  °C per  
50 decade and 6.8% a cooling of  $-0.11 \pm 0.10$  °C per decade. Increase in SST is especially  
51 important in coastal areas due to its strong impact in coastal ecosystems (Honkoop et al., 1998;  
52 Burrow et al., 2011; Wernberg et al. 2016). Simultaneously, coastal SST is highly influenced  
53 by local factors, such as the anthropogenic land-based processes, upwelling currents, fresh  
54 water discharge, ocean fronts and local tidal mixing. An accurate analysis of the local SST  
55 and its variability is needed for marine ecosystem-based management. Here, we mainly focus  
56 on three globally gridded SST datasets, that is, the HadISST1, ERSST, COBE SST (Rayner et  
57 al., 2003, Ishii et al., 2005, Smith et al., 2008, Hirahara et al., 2014; Huang et al., 2015).  
58 Besides, a fourth SST product is considered, i.e., NOAA Optimum Interpolation SST (OISST)

59 version 2 using Advanced Very High Resolution Radiometer infrared satellite SST data from  
60 the Pathfinder satellite combined with buoy data, ship data, and sea ice data, covering from  
61 1982 to present. Because of its high spatial resolution of  $0.25^{\circ} \times 0.25^{\circ}$ , it is used in the  
62 concluding section for clarifying some additional aspect. All of these datasets have been  
63 widely used in the regional and global climate change studies. Given that these datasets have  
64 been developed by independent groups, there are some differences of data sources, bias  
65 adjustment and reconstruction method, etc. in the SST analyses products. For example, some  
66 analyses only use in situ observations, such as ERSST v4 and COBE SST. Others use both in  
67 situ and satellite observations, such as OISST and HadISST1. There are also some differences  
68 from quality control and gap-filling choices when and where observations are sparse,  
69 particularly in early record periods and coastal areas (Huang et al., 2015; Li et al., 2017).  
70 These differences also indicate some uncertainties in these SST analyses. In order to test the  
71 validity of these gridded SST datasets along the coast of China, SST records for the period of  
72 1960–2015 at total 26 Chinese coastal hydrological stations coast are used. All of these *in situ*  
73 SST data from 1960 to 2015 are provided by the National Marine Data and Information  
74 Service (NMDIS) of China and have been quality controlled and homogenized by Li et al.  
75 (2018). These SST data from coastal hydrological stations have never been merged into  
76 HadISST, COBE SST or other gridded SST analyses. Therefore, the homogenized long-term  
77 SST observations along the Chinese coast can be used for evaluation on these analyses. We  
78 study the performance of these gridded SST datasets in the coastal waters by comparing to the  
79 homogenized SST.

80 Thus, the remainder of this paper is structured as follows: Details on the observational and  
81 gridded data sets and methodology used in this study are given in section 2. Section 3  
82 introduces the local homogenized SST series along the Chinese coast (Li et al., 2018), which  
83 is used as a reference to compare to the gridded data sets with. For adding confidence in the  
84 quality of this local SST data set, these SST data are compared with an independently  
85 constructed local air temperature data. The basic statistics of the local SST-data series are also  
86 shown. Section 4 describes the results and comparisons with gridded SST data sets in the  
87 Chinese coastal waters. Further discussion and conclusion are given in section 5.

## 88 **2. Data and methodology**

### 89 **2.1. Data source**

90 The SST records during 1960–2015 at the 26 sites of coastal hydrological stations along the  
91 Chinese coast have been assembled and homogenized. Homogenized monthly mean surface

92 air temperature (SAT) series from National Meteorological Information Center (NMIC) of  
 93 China (Xu et al., 2013) and the gridded SAT from the latest version of the Climate Research  
 94 Unit's (CRU) gridded high resolution (0.5°×0.5°) dataset CRU TS 3.24.01 for 1960–2015  
 95 (Harris et al., 2014) are used to investigate the consistency of homogenized SST data with the  
 96 local SAT.

97 Four globally gridded SST datasets are used in our work (see Table 1): (1) The 1°×1° Hadley  
 98 Center Sea Ice and Sea Surface Temperature monthly dataset (HadISST) (Rayner et al., 2003);  
 99 (2) The 1°×1° Centennial In Situ Observation-Based Estimates of the Variability of SST  
 100 (COBE SST) (Hirahara et al., 2014); (3) 2°×2° Extended Reconstructed Sea Surface  
 101 Temperature version 4 (ERSST v4) for 1960–2015 (Smith et al., 2008, Huang et al., 2015). (4)  
 102 NOAA OISST v2 for 1982–2015 (Reynolds et al. 2007).

103 **Table 1.** Global gridded SST datasets that are used in this study

Dataset	Resolution	Period	Sources
ERSST v4	2°x 2°	1960– 2015	<a href="http://www.ncdc.noaa.gov/oa/climate/research/sst/ERSST.v4.php">http://www.ncdc.noaa.gov/oa/climate/research/sst/ERSST.v4.php</a>
HadISST	1°x 1°	1960– 2015	<a href="http://www.metoffice.gov.uk/hadobs/hadisst/data/download.html">http://www.metoffice.gov.uk/hadobs/hadisst/data/download.html</a>
COBE SST	1°x 1°	1960– 2015	<a href="http://ds.data.jma.go.jp/tcc/tcc/products/elnino/cobesst/cobe-sst.html">http://ds.data.jma.go.jp/tcc/tcc/products/elnino/cobesst/cobe-sst.html</a>
OISST	$\frac{1}{4} \circ \times \frac{1}{4} \circ$	1982– 2015	<a href="http://www.ncdc.noaa.gov/oisst">http://www.ncdc.noaa.gov/oisst</a>

## 104 2.2. Methodology

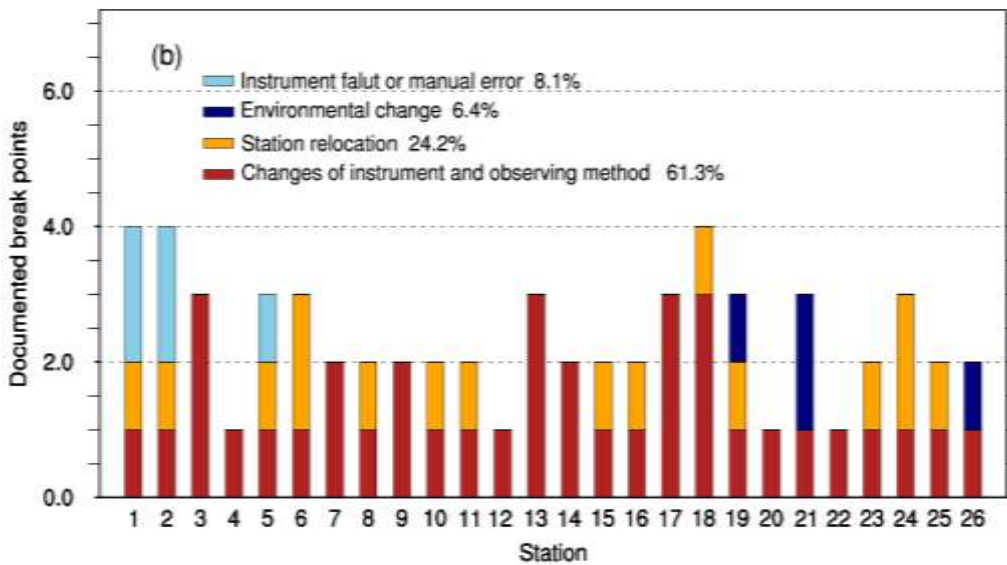
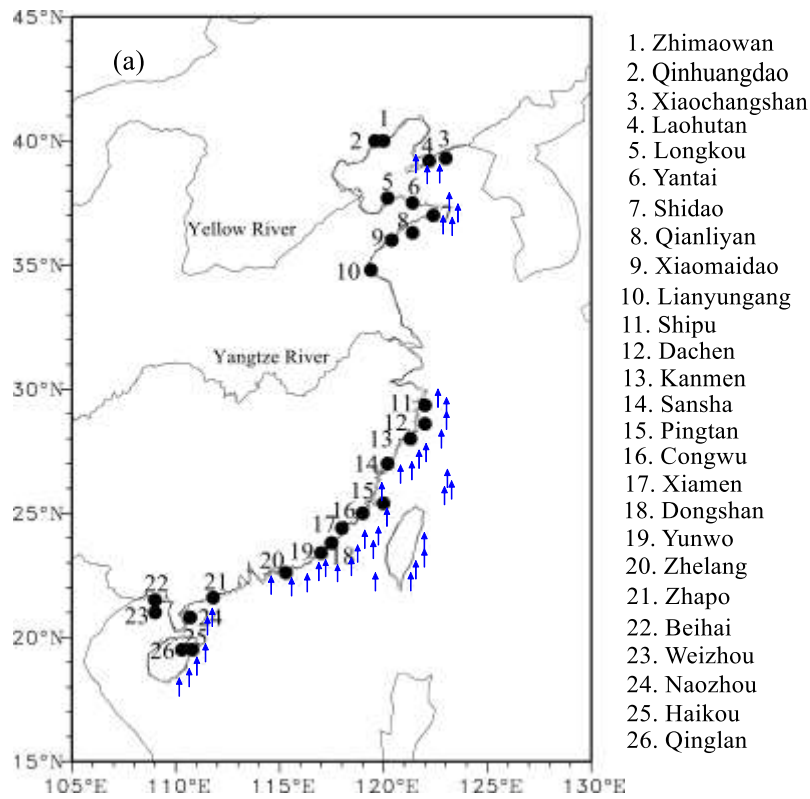
105 Statistical methods such as conventional empirical orthogonal function (EOF) (Kim et al.,  
 106 1996, von Storch and Zwiers 1999), correlation analysis and linear trend analysis are  
 107 employed. The significance of each trend has been tested by the Mann-Kendall test using  
 108 Sen's slope estimates quantify trends (Sen, 1968). The tests were stipulated to operate with a  
 109 probability for a false rejection of the null hypotheses (i.e., zero trend) of 5%. They are  
 110 conducted with the implicit assumption that the data are serially independent. There are only  
 111 weakly correlated but not really independent. Thus, the tests are “liberal”, i.e., have  
 112 tendencies for falsely rejecting too often the null hypothesis, when it is actually valid (von  
 113 Storch and Zwiers, 1999). However, since the effect is relatively weak, given the small serial  
 114 correlations, and since we have no results, which are close to the stipulated critical levels, we

115 do as if the serial dependence is not of importance. However, this caveat should be kept in  
116 mind, when assessing the results.

### 117 **3. The local homogenized SST records along the Chinese coast**

118 Currently, more than 100 coastal hydrological stations are operating and monitoring near-  
119 shore hydrological conditions. Among these stations, only 26 stations have routinely and  
120 continuously recorded since 1960, with a percentage of missing data less than 4%. Also, these  
121 stations have undergone only a few (five or less) documented relocations. The locations of the  
122 26 coastal hydrological stations are shown in Fig.1a. Due to the fact that this area between  
123 29 N (Station 11) and 35 N (Station 10) is a vast muddy coast which is not suitable for  
124 hydrological stations, there are only 10 hydrological stations. Among them, some stations  
125 were built up after 2000s and some have much missing data. That is why no station has been  
126 chosen between 29 N (Station 11) and 35 N (Station 10). Monthly mean SST series were then  
127 derived and subjected to a statistical homogeneity test, called the Penalized Maximum T  
128 (PMT) test (more details can be found in Li et al., 2018). Homogenized monthly mean SST  
129 series were obtained by adjusting all significant change points which were supported by  
130 historic metadata information. These identified change points at each station are displayed in  
131 Fig.1b. The majority of change points are caused by instrument changes and station  
132 relocations, accounting for 60.6% and 24.6% of the total, respectively. In our work, we  
133 consider annual mean values. Some analyses with seasonal mean values are also calculated,  
134 but these are not covered by our present account and merely summarized. The supporting  
135 evidences are provided by the Supplementary Online Material (SOM) in Appendix B.

136 The standard statistics derived from the data in the period of 1960–2015, that is, long-term  
137 mean, the standard deviation of annual means and the decadal trends are listed in Table 2.  
138 SSTs vary along the Chinese coast, between about 11.5 °C at the north and 25 °C at the  
139 southernmost locations. The standard deviations are of the order of 0.50 °C at all locations,  
140 with a maximum of 0.71 °C and a minimum of 0.43 °C. The decadal trends vary between 0.13  
141 °C per decade to 0.29 °C per decade. Table 2 also provides the long-term means of the  
142 homogenized data and of the raw (unhomogenized) data. The differences between the  
143 homogenized data and the raw data (last column) vary between -2.26 K and 0.53 K. At 22 of  
144 the 26 stations, a downward correction of the mean has been found necessary – only at Station  
145 15 (Pingtan) and Station 23 (Weizhou) an upward change was stipulated, and in two case  
146 nearly no change of the mean at Station 7 (Shidao) and Station 24 (Naozhou).



150 **Figure 1.** Study area and locations of 26 coastal sites (a), for which continuous monthly SST recordings are  
 151 available and corrected by eliminating inhomogeneities. The number of identified breakpoints in individual  
 152 SST stations from 1960–2015 (b). Result from Li et al. (2018). Black circle represents 26 coastal sites and  
 153 blue arrow represents coastal upwelling.

155 **Table 2.** Statistics of the time series of the annual homogenized local SST, plus the differences to the raw  
 156 data, which were used to construct the homogenized series (columns 6 and 7).

Station No.	Full name	Mean homogenized SST	Standard deviation	Trend ( °C/10yrs)	Mean unhomogenized SST	Diff
1	Zhimaowan	11.50	0.53	0.17	11.75	-0.25
2	Qinhuangdao	12.21	0.59	0.26	12.32	-0.11
3	Xiaochangshan	11.54	0.71	0.29	11.73	-0.19
4	Laohutan	11.36	0.59	0.21	11.47	-0.11
5	Longkou	13.36	0.59	0.22	13.51	-0.15
6	Yantai	12.65	0.59	0.17	12.79	-0.14
7	Shidao	12.09	0.59	0.14	12.08	0.01
8	Qianliyan	14.37	0.65	0.17	14.41	-0.04
9	Xiaomaidao	13.76	0.63	0.22	13.84	-0.08
10	Lianyungang	14.85	0.57	0.21	14.94	-0.08
11	Shipu	17.41	0.65	0.26	18.01	-0.61
12	Dachen	17.67	0.65	0.24	17.91	-0.24
13	Kanmen	18.20	0.56	0.17	18.42	-0.22
14	Sansha	19.21	0.71	0.21	19.91	-0.19
15	Pingtang	19.72	0.61	0.19	19.45	0.53
16	Congwu	19.98	0.52	0.17	22.18	-0.64
17	Xiamen	21.50	0.51	0.19	21.47	-2.26
18	Dongshan	20.84	0.45	0.13	21.12	-0.28
19	Yunwo	21.02	0.44	0.13	21.36	-0.34
20	Zhelang	22.43	0.44	0.15	22.62	-0.19
21	Zhapo	23.62	0.50	0.18	23.68	-0.06
22	Beihai	23.60	0.55	0.18	24.06	-0.46
23	Weizhou	25.79	0.43	0.17	25.66	0.13
24	Naozhou	24.46	0.49	0.16	24.44	0.02
25	Haikou	25.00	0.49	0.16	25.10	-0.10
26	Qinglan	25.80	0.44	0.18	25.86	-0.07

157

158 The quality of the data set has already been documented by Li et al. (2018). To add  
159 confidence in the quality of this data set, we compared the new data set to an independent data  
160 set of local SAT at 26 nearby local stations. Also, this data set has been homogenized –  
161 independently of the processing of the SST series. SST and SAT data are not compares  
162 directly pairwise, but in terms of the patterns and coefficient time series (PCs) of their EOFs.  
163 The similarity of the principal components is striking. The first PCs share a correlation  
164 coefficient of 0.97, and the second 0.86 (Fig.A1). Thus, the SST series are fully consistent  
165 with these SAT series. When this exercise is repeated with CRU TS 3.24.01 instead of the in-

166 situ SAT series, we find a similar consistency (see Fig. SOM-1). The PCs of SAT-CRU also  
167 show high correlations of 0.94 and 0.83 with the in situ SST (see Fig. SOM-1) (more details  
168 are shown in Appendix A and B). Thus, we conclude that our homogenized SST data is  
169 superior to earlier used data on the SST variability and trends along the Chinese coast.

#### 170 **4. Comparison with gridded SST datasets in the Chinese coast waters**

171 Given the consistency of the newly homogenized SST series with independent regional SAT  
172 data, we use it as a benchmark for assessing the regional quality of the four globally gridded  
173 SST data sets in Table 1. In the following, we name the new data set “Local homogenized  
174 SST” as “LH”, while the datasets extracted from the gridded SST datasets as “localized  
175 analysis data”, and use the abbreviation “LA”. For instance, LA-HadISST is the SST found in  
176 HadISST in the local grid box, which contains the locations in the LH data set.

177 These “localized” time series (LA) of the three gridded datasets, which extend to the full time  
178 window 1960–2015 (ERSST, HadISST, COBE SST; referred as LA-ERSST, LA-HadISST,  
179 LA-COBE SST) are then compared to the local series — LH, by first comparing the standard  
180 deviations and the trends, and by calculating from trends, differences (Diff) and the root mean  
181 square errors (RMSEs) for the 26 stations (Table 3). We do this for annual mean values. The  
182 fourth dataset, OISST data, covers a shorter time window from 1982–2015 and has a high  
183 spatial resolution. It is used in the concluding section for clarifying some additional aspects in  
184 the section 5.

185 For summarizing the results, we compute EOFs of the LH and the LAs, as well as for the  
186 differences of LH and LAs. The LH data are derived from observational stations, whereas the  
187 LA data are representing area values averaged across a grid box. Therefore, the LA data  
188 should vary less than the LH data. Possible mismatches between the local LH data and the  
189 spatial averages of grid box data in the LAs may be related to small scale effects; however,  
190 the usage of EOFs is expected to reduce these truly local specifics, as the first EOFs describe  
191 joint co-variations among the 26 elements in both LA and LH data sets.

#### 192 **4.1. Comparing with HadISST**

193 The 56-year mean values of local SST in the analysis LA-HadISST are in all cases higher than  
194 at the local stations (Table 3). Some differences are of the order of 2K and even 3K, in  
195 particular along the East China Sea extending from Station 11 (Shipu) to Station 20 (Zhelang).



196 To some extent, this difference may reflect differences between averages of a larger coastal  
 197 ocean area and *in situ* observations, but not entirely.

198 The variations in LA are similar to LH, but there are some differences: as expected, 65.4% of  
 199 the standard deviations (17) are larger for LH, and 34.6% cases (9) smaller. The correlations  
 200 are all large enough to reject the null hypothesis of the absence of a link (if we assume serially  
 201 independence the 90%-critical value is 0.22) except for the northernmost Station 19 (Yunwo).  
 202 Part of the difference to the ideal value of 1 may be due to the different spatial scale, but  
 203 values as low as 0.41 indicate to more systematic differences. The trends are positive for all  
 204 sites (Table 3) – only the northernmost Station 1 (Zhimaowan) signals a weak downward  
 205 trend in the LA-HadISST data set. In about 50% of the case, the coastal sea warms faster  
 206 according to LH than to LA-HadISST, and for 50% it is the opposite. For the two  
 207 northernmost sites, Station 1 (Zhimaowan) and Station 2 (Qinhuangdao), the warming  
 208 according to LA is very weak, whereas along the stretch from Station 15 (Pingtan) to Station  
 209 19 (Yunwo) the warming according to LA-HadISST is considerably stronger than in LH.

210 The time series for the two northern sites in the Bohai Sea are shown in Fig. 2. The sequence  
 211 of maxima and minima share some similarity, but the trends differ markedly. The LH curves  
 212 (red lines) exhibit both a steady increase, whereas the LA-HadISST curves (black lines) tend  
 213 to decline in the first 10–20 years, and to vary at a mostly constant level (Fig.2a and 2b). In  
 214 this case, the “story told” by LH is considerably different than that of LA-HadISST.

215 The time series of the SST averaged across the stations from Station 15 (Pingtan) to Station  
 216 19 (Yunwo) along the East China Sea coast, where LA-HadISST indicated a stronger  
 217 warming than in the LH, is shown in Fig. 2c. The local data indicate markedly lower  
 218 temperatures, which may mainly be because of coastal upwelling (the effect of upwelling will  
 219 be discussed in the Section 5), but also other local effects, including local tidal mixing, ocean  
 220 fronts, sea water vertical mixing, and fresh water discharge, etc., but also a weaker trend (0.18  
 221 °C per decade) than in the LA-HadISST (0.35 °C per decade).

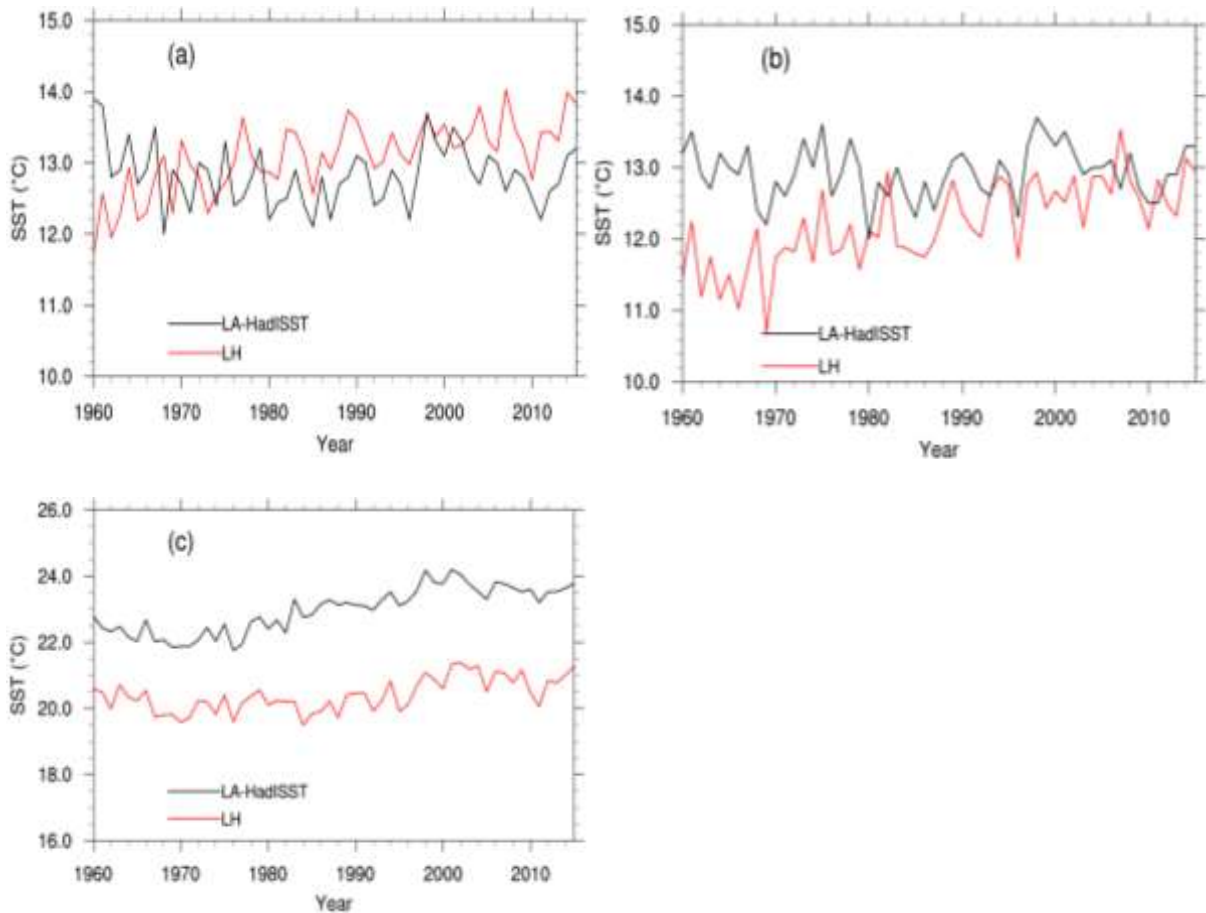
222 **Table 3.** Statistics of the time series of the localized SST-analysis (LA-HadISST) data series at the 26  
 223 station, as well as the differences (Diff) between statistics of the LH series given in Table 1. The correlation  
 224 coefficients between LH and LA-HadISST are also calculated (the 90% confidence level is 0.22, without  
 225 considering serial correlation). Red numbers indicate that the correlation coefficients do not conflict with  
 226 the null hypothesis of no correlation.

Station	Mean	Diff	Std deviation	Diff	Trend	Diff	Corr
---------	------	------	---------------	------	-------	------	------

No.	LA-HadISST		LA-HadISST		( °C/10yrs)		
1	12.80	-1.32	0.43	-0.06	-0.02	0.25	<b>0.20</b>
2	12.93	-0.72	0.37	0.21	0.02	0.24	0.31
3	13.45	-1.76	0.46	0.38	0.13	0.16	0.73
4	13.86	-2.30	0.51	0.07	0.15	0.07	0.67
5	13.71	-0.24	0.54	0.28	0.11	0.11	0.66
6	13.92	-1.12	0.57	0.01	0.14	0.03	0.69
7	14.87	-2.58	0.58	0.01	0.19	-0.05	0.70
8	14.51	0.01	0.54	0.10	0.14	0.03	0.77
9	14.51	-0.60	0.54	0.08	0.14	0.08	0.66
10	16.05	-1.07	0.47	0.10	0.21	0.00	0.71
11	19.70	-2.00	0.57	0.08	0.12	0.14	0.63
12	20.66	-2.65	0.59	0.05	0.27	-0.03	0.67
13	20.66	-2.12	0.59	-0.03	0.27	-0.10	0.64
14	22.47	-2.30	0.70	0.01	0.35	-0.14	0.73
15	23.43	-3.00	0.75	-0.14	0.34	-0.15	0.65
16	23.43	-1.45	0.77	-0.25	0.40	-0.23	0.75
17	22.03	-2.41	0.77	-0.26	0.40	-0.21	0.78
18	24.46	-3.26	0.59	-0.14	0.30	-0.17	0.59
19	24.46	-3.08	0.59	-0.15	0.30	-0.17	0.66
20	25.44	-2.82	0.46	-0.02	0.20	-0.05	0.83
21	25.66	-1.78	0.51	-0.01	0.07	0.11	0.56
22	25.11	-1.47	0.31	0.24	0.07	0.11	0.53
23	25.11	0.71	0.31	0.13	0.07	0.10	0.41
24	25.65	-1.02	0.40	0.09	0.19	-0.03	0.55
25	25.65	-0.47	0.40	0.09	0.19	-0.03	0.57

227

26	25.93	0.09	0.43	0.00	0.22	-0.04	0.64
----	-------	------	------	------	------	-------	------



228

229

230 **Figure 2.** The annual mean SST series of LA-HadISST (black line) and LH (red line) from Station 1  
 231 (Zhimaowan) (a) and Station 2 (Qinhuangdao) (b); The average annual mean SST series of LA-HadISST  
 232 (black line) and LH (red line) from Station 15 (Pingtan) to Station 19 (Yunwo) (c).

233

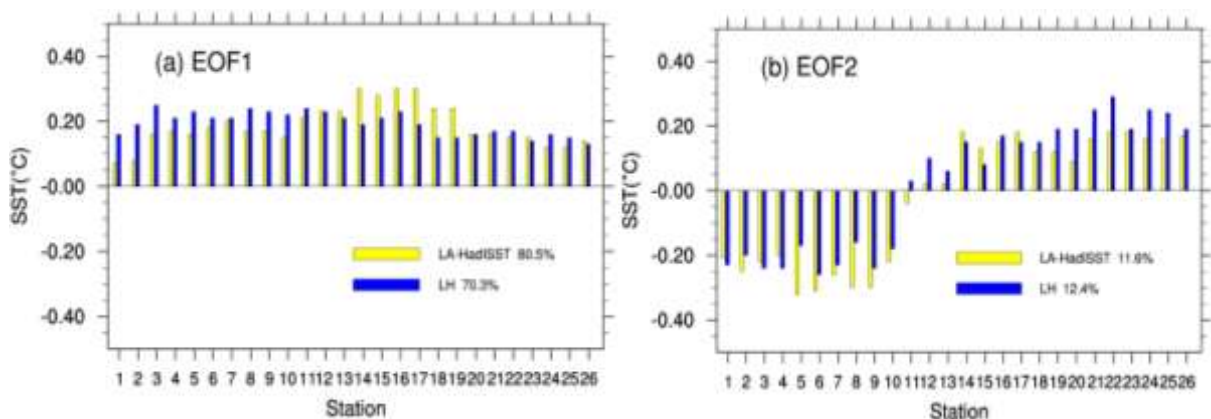
234 The first two EOFs of the LH and the LA data set have similar patterns, namely a uniform  
 235 sign along the entire coast in EOF1, with similar intensities, and a north-south dipole (Bohai  
 236 Sea and Yellow Sea vs. East and south China Sea) in EOF2, with a sign change at Station 11  
 237 (Shipu) (Fig.3a and 3b). The two patterns of LH explain less variance, namely 82.9% of the  
 238 total variance, than the LA-HadISST EOFs, which go with 92.9%. This may be related to the  
 239 larger spatial variability in local data compared to gridded data. In EOF1, again the Station 1  
 240 (Zhimaowan) and Station 2 (Qinhuangdao) in the Bohai Sea contribute less in LA-HadISST,  
 241 whereas the Station 15 (Pingtan) to Station 19 (Yunwo) contribute more to the overall  
 242 warming than in LA-HadISST than in LH.

243 The time coefficients (PCs) are broadly similar, even if the correlations are not very strong:  
 244 only 0.84 and 0.42 (Fig.3c and 3d). A general warming is associated with EOF1 and mostly  
 245 stationary inter-annual variability with EOF2. Again, the sequence of maxima and minima is

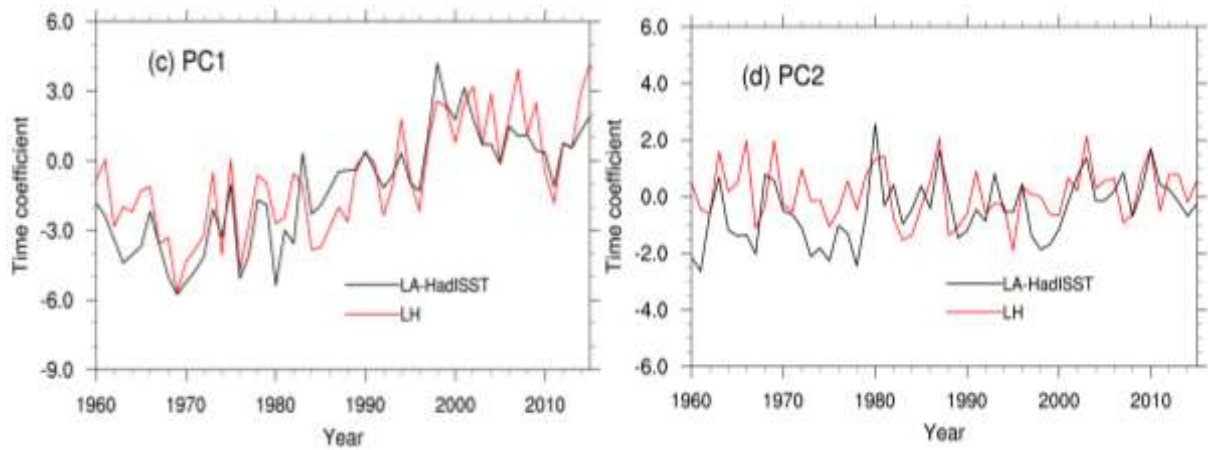
246 qualitatively similar, but PC2 of LA-HadISST exhibits a break point at about 1980 –  
 247 interestingly the time when satellites became routinely available of the global analyses. These  
 248 data improve SST sampling, especially in the Southern Ocean and coastal areas (Smith et al.,  
 249 2008; Lima and Wetthey 2012). Before 1980, PC2 of LH and LA-HadISST differed by about  
 250 0.2 (Fig. 3d; this corresponds to a mean difference of 0.04K at the southern stations from  
 251 Station 11 to Station 26 during that time, and a mean difference 0.04K at the northern stations  
 252 from Station 1 to Station 10 (Fig. 3b)).

253 To further study the differences in trends, EOFs were calculated from the difference time  
 254 series, that is, LH anomalies minus LA-HadISST anomalies at the 26 sites (Fig. 4). The first  
 255 two EOFs stand for 31.2% and 27.6% of the variance. These numbers are not very different,  
 256 and it their closeness may be indicative that the EOFs are degenerate (von Storch and Zwiers  
 257 1999). These EOFs describe covariations of the differences along long stretches of the coast;  
 258 in case of EOF1, this is the case for all stations at the southern Station 11 (Shipu), i.e., in the  
 259 East and South China Sea (Fig.4a). In EOF2 it is all stations at the southern Station 13  
 260 (Kanmen), mostly in the Yellow Sea and Bohai Sea (Fig. 4b). PC1 seems to describe a change  
 261 point at about 1980, whereas PC2 describes a slight upward trend: The differences tend to be  
 262 larger in earlier years and are almost nil in the end of the considered time interval. That is, in  
 263 recent years, there are little differences between LA-HadISST and LH, which is not surprising  
 264 giving the better observational and reporting practice.

265 That in early years inhomogeneities impacted the quality of SST analyses is also not  
 266 surprising, but it is valuable to learn when these inhomogeneities took place, and which time  
 267 periods in the analyses should be taken with some reservation. Of course, this assertion  
 268 depends on the assumption that the homogenization of the local data did remove all change  
 269 points and other inhomogeneities.



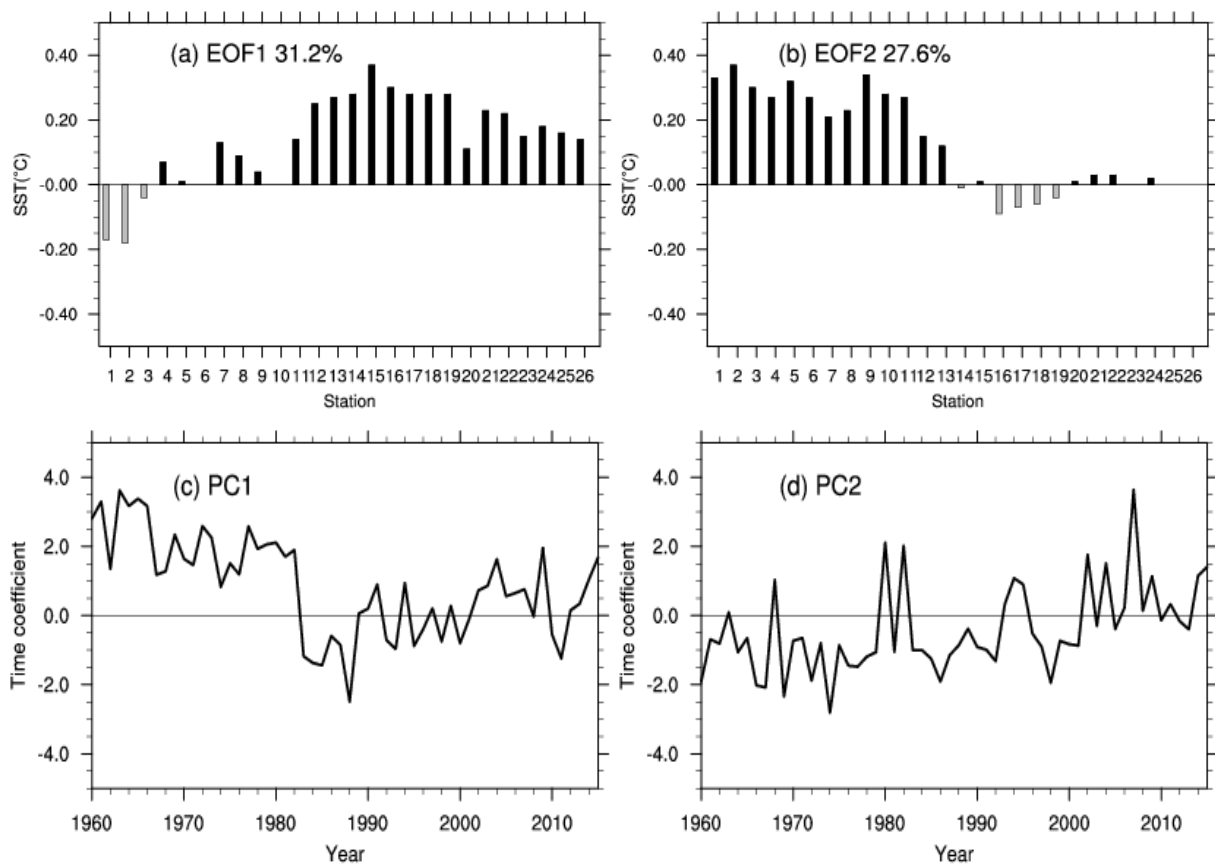
270



271

272 **Figure 3.** Comparison of the EOF1 and EOF2 derived from the LH data set of local SST at 26 sites (blue  
 273 bars; red lines), and derived from the localized analysis data LA-HadISST (yellow bars; black lines).  
 274 Top: EOF spatial patterns, bottom: principal components (time coefficients).

275



276

277 **Figure 4.** First two EOFs of the difference time series LH-LA-HadISST. Top: EOF spatial patterns, bottom:  
 278 principal components (time coefficients).

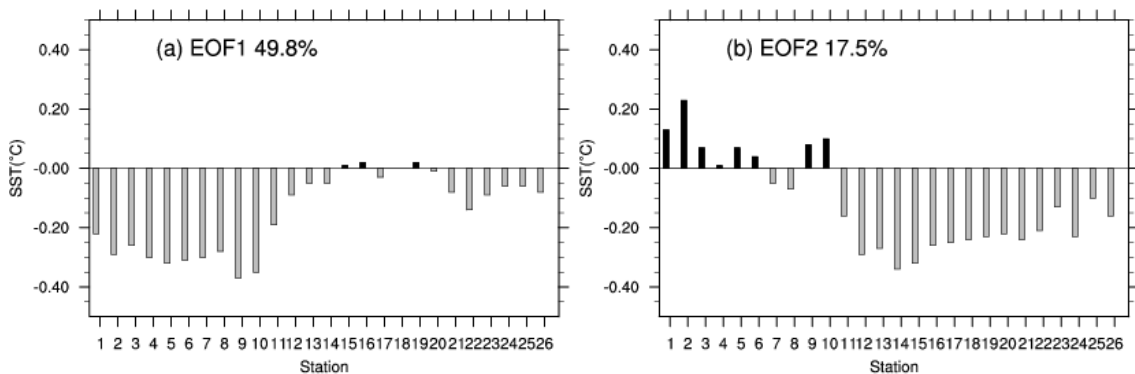
279

## 280 4.2 Comparing with COBE SST

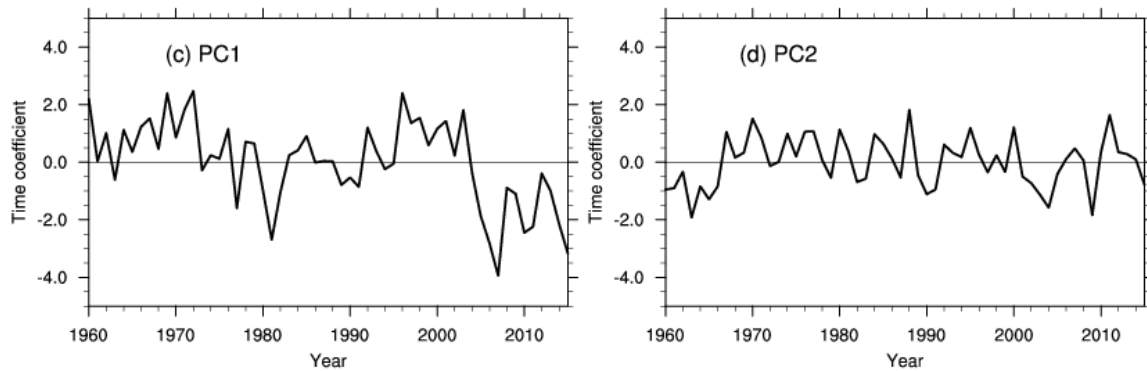
281 In this subsection, we consider the localized SST derived from the LA-COBE SST data set  
282 during 1960–2015. Again, the LA-COBE SST is in almost all sites higher than the local data,  
283 namely at 21 out of 26 sites. The differences are up to 3K, and again mostly along the East  
284 China Sea coast from Station 11 (Shipu) to Station 20 (Zhelang) (see Table SOM-1 in the  
285 Supplementary Online Material (SOM)). The local correlations are relatively high, namely  
286 between 0.55 and 0.85.

287 The EOFs derived from the LA-COBE SST, with the same grid resolution of  $1^\circ$  and the same  
288 time window 1960–2015 as LA-HadISST, exhibits broadly the same pattern in space and time  
289 as the EOFs of the LH data. Also, the explained variances are close (Figure SOM-2). The  
290 northern stations contribute more to the overall warming represented by EOF1, whereas the  
291 stations along the South and East China Sea contribute less. Again, the two northernmost  
292 Station 1 (Zhimaowan) and Station 2 (Qinhuangdao) exhibit some systematic differences,  
293 both in EOF1 and EOF2. The PCs share correlations of 0.80 for EOF1 and 0.50 for EOF2.  
294 COBE SST does not capture the recovery of the dip in warming since about 2000, as LH and  
295 HadISST did, while EOF2 reveals some warming in the final years. During the 1960s some  
296 differences prevail.

297 Fig.5 shows the EOFs of the difference time series between LH anomalies and LA-COBE  
298 SST anomalies. The first EOF dominates, with 49.8%, whereas the second one represents a  
299 share of 17.5%. The first EOF points to several inhomogeneities, with two prolonged intervals  
300 during which LH is higher than LA-COBE SST (i.e., 1960–1978, and 1995–2005), and a  
301 strong drop-down to negative PC-values after about the year of 2005. PC2, on the other hand,  
302 appears as mostly stationary, except for a suspiciously negative episode in the early 1960s.



303



304

305 **Figure 5.** EOF analysis of the differences LH-LA-COBE: Top: EOF spatial patterns (EOFs), bottom:  
 306 principal components (time coefficients).

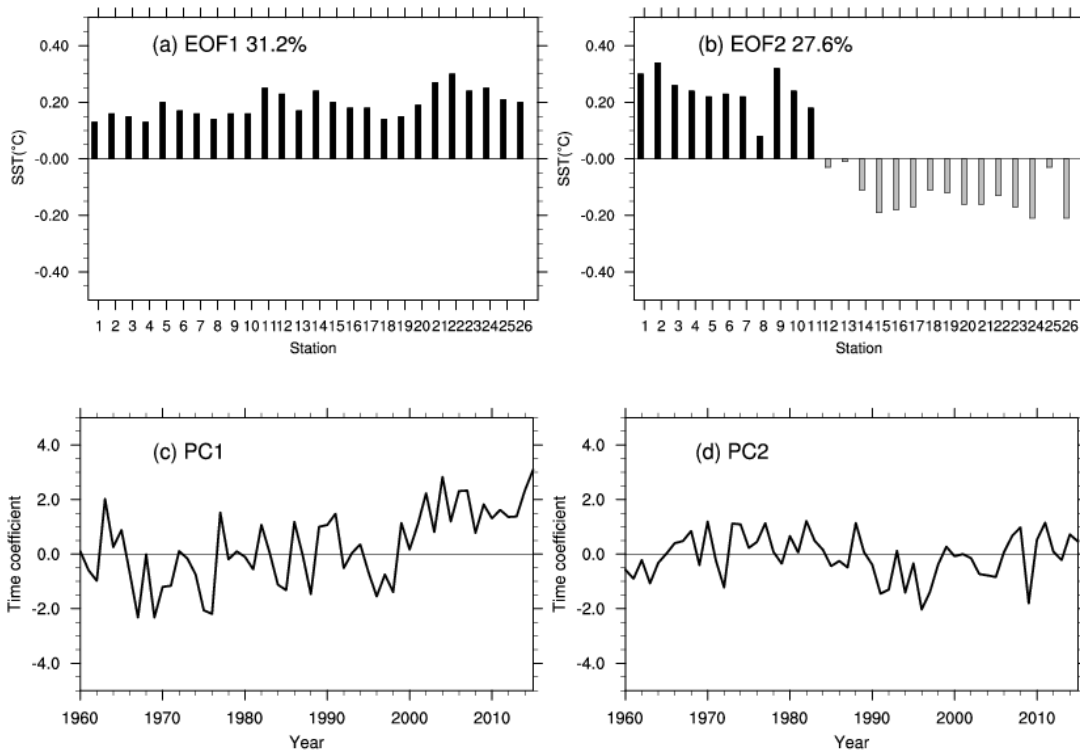
### 307 **4.3 Comparing with ERSST**

308 ERSST presents SST on a coarser grid compared to the two cases before. Again, the  
 309 temperatures given by ERSST, as was the case with the other two analyses, are higher than  
 310 the temperatures recorded at the local sites along the coast (see Table SOM-2). The  
 311 differences are up to 4K, and the largest differences are found in the East China Sea from  
 312 Station 11 (Shipu) to Station 20 (Zhelang). That the differences are in this case even larger  
 313 than in the other LA cases may be related to the 2° coarse resolution of ERSST.

314 The variability according to ERSST is quite similar to that of LH, at least in terms of EOFs  
 315 (see Figure SOM-3). The correlation of the PC1's is 0.83, and of PC2's to 0.60. LA-HadISST  
 316 got 0.84 and 0.42, LA-COBE SST got 0.80 and 0.50. The local correlations vary between 0.37  
 317 and 0.82. Again EOF1 stands for an overall warming and EOF2 to interannual variability with  
 318 hardly a trend. The relative contributions of the two EOFs compare well to the LH-EOFs. In  
 319 detail, the northernmost stations appear stronger in EOF1 of LA-ERSST than in that of LH,  
 320 whereas the northern sites are underrepresented, and the southern over-represented in EOF2.

321 The EOFs of the differences between LH anomalies and LA-ERSST anomalies are shown in  
 322 Fig. 6. They differ strongly from those found for LA-COBE SST and LA-HadISST. The first  
 323 EOF differences resemble the first EOFs of LH and LA-ERSST (not shown; see Fig. SOM-3)  
 324 – the long-term trend in LA-ERSST is smaller than in the local data – everywhere. The  
 325 second EOF is again a dipole pattern, with the Bohai Sea and the Yellow Sea on the one side,  
 326 and the East China Sea and South China Sea on the other. The time series of PC2 fluctuates  
 327 around zero without prominent long-term trend.





328

329

330 **Figure 6.** EOF analysis of the differences LH-LA-ERSST: Top: EOF spatial patterns (EOFs), bottom:  
 331 principal components (time coefficients).

332

### 333 **5 Discussion and conclusion**

334 We have mainly examined three global gridded analysis SST data sets in the Chinese coastal  
 335 waters. For doing so, we have compared a number of statistical properties for 26 coastal  
 336 hydrological locations as given by the analyses and by a newly digitized and homogenized  
 337 data set (Li et al., 2018). For demonstrating the utility of the local data set, we have compared  
 338 the local SST series (named LH) with independent local homogenized SAT data from nearby  
 339 meteorological stations. The variations of the two series are fully consistent. Another  
 340 argument points to the quality of the LA data set is that the differences between LH and the  
 341 three LAs (localized data from the different global analyses: HadISST1, COBE SST, ERSST)  
 342 considered are not uniform (except for the time mean); instead the LAs deviate in different  
 343 ways from LH. If this would not be the case, one could be tempted to argue that the  
 344 differences are manifestations of inefficiencies of the LH data set. This is not the case.

345 In this study, we found that all of these globally gridded datasets exhibit surface temperatures  
 346 usually higher than the LH data, especially at the East China Sea. This difference may be  
 347 caused by two factors. In the China Seas, most of the coastal upwelling currents occur at the  
 348 East China Sea and the northern South China Sea, other small upwelling currents at the tops

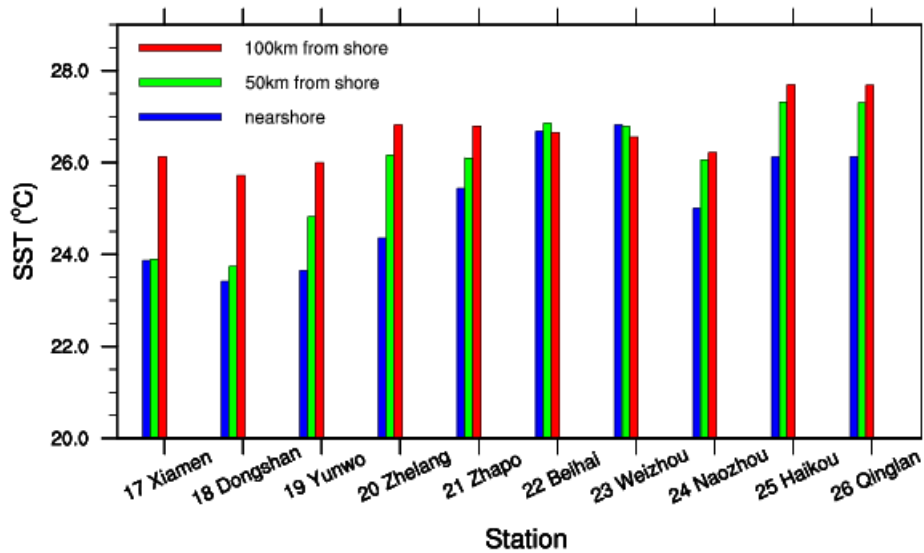
349 of the Liaodong Peninsula and Shandong Peninsula (Figure 1) (Yan 1991). The consensus of  
350 previous studies is that coastal upwelling currents results in cooling SST at these coastal areas  
351 (Xie et al, 2003; Guan et al., 2009; Su et al., 2012). In our study, we find that the in-situ  
352 shoreline SSTs at the upwelling areas (e.g. Station 4 (Laohutan), Station 11 (Shidao) and  
353 Station 18 (Dongshan)) are always colder than global gridded SST data, with the value of  
354 below -1K (Table 2, Table 3 and Table SOM1).

355 We hypothesize that these negative differences are connect by coastal upwelling currents. To  
356 test this hypothesis, we examine the output of a numerical simulation of the currents in the  
357 South China Sea with a grid resolution of  $0.04^\circ$ . The model is embedded in an almost global  
358 model with  $1^\circ$  grid resolution (Tang et al., 2018). The model used here is the Hybrid  
359 Coordinate Ocean Model (HYCOM) that is exposed to periodic climatological atmospheric  
360 forcing, with a fixed annual cycle but no weather disturbances. The atmospheric forcing  
361 comes from the International Comprehensive Ocean-Atmosphere Data set (ICOADS). We  
362 extract simulated SSTs at three different distances (i.e., near the station, 50 km, and 100 km  
363 from each coastal hydrological station in South China Sea). Fig.7 shows that most shoreline  
364 SSTs are lower than ambient offshore SSTs, especially SSTs at 100km from shoreline.  
365 However, the Stations 22 (Beihai) and Station 23 (Weizhou) are not affected by coastal  
366 upwelling, and consistently, there are no notable differences among SSTs at three different  
367 distances from the two stations. The result reflects that the homogenized SST data set for  
368 shoreline stations catches this relative cooling water effect of the regional upwelling currents.  
369 On the other hand, the global gridded SST datasets point to higher temperatures which may be  
370 caused by their coarse resolution. The differences are largest in the case of the coarsest  
371 analysis (ERSST), but weakest in the OISST v2 analysis with a resolution of  $0.25^\circ$  (Fig. 8; see  
372 below) (Note that the difference of LH minus LA-OISST is restricted to the warmer episode  
373 1982–2015). Meanwhile, the lack of near-shore observations when compiling near-shore box  
374 averages in coastal areas may also cause these differences (Wang et al., 2018). Besides, there  
375 still some other local mechanisms with smaller scale can cause cooling water in the China  
376 Seas, such as China coastal current (CCC) (Belkin and Lee, 2014) and ocean fronts (Zhao,  
377 1987; Hickox et al., 2000). In them, the shallow water shelf front and estuarine plume front  
378 are two major fronts in the Bohai Sea and the Yellow Sea in summer. Coastal current front,  
379 upwelling front as well as strong westerly boundary current usually appears in the East China  
380 Sea and the South China Sea which may also be related to coastal upwelling currents.

381 In summary, our main results are as follows:

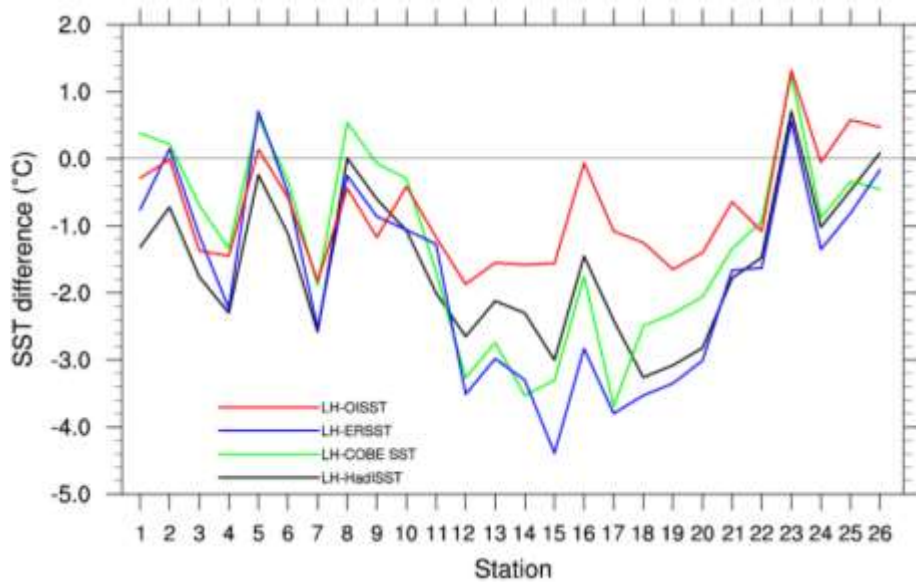
- 382 – The mean SST in LH at many sites is considerably lower than that in the LA-data sets.  
383 We suggest that this is related to local oceanic effects, such as coastal upwelling. The  
384 LA-datasets cannot catch this cooling effect of the regional upwelling currents well.  
385 On the other hand, the global gridded SST datasets point to higher temperatures which  
386 may be caused by their coarse resolution when averaging in the LA data sets. However,  
387 systematic differences would not be expected to influence strongly the overall  
388 variability and trends.
- 389 – The first EOF in all data sets stands for a general warming, and the second for  
390 interannual variability. This is not only so in the local LH-data but also in all globally  
391 gridded-based LA-datasets.
- 392 – In the years following the introduction of satellites in monitoring SST, since about  
393 1980, the different global analyses converge, and the differences to the local data set  
394 become smaller. In support of this, the comparison with the high resolution analysis  
395 OISST v2 for the post-satellite period 1982–2015 reveals few differences (not shown,  
396 see Fig. SOM-4).
- 397 – In the years before 1980, some noteworthy differences are found. The differences  
398 between the LH-data anomalies and the LA-data anomalies are non-uniform across the  
399 different LA data sets. For instance, for ERSST the long-term trends differ, in case of  
400 COBE SST several jumps emerge, and in case of HadISST, a jump is found at the time  
401 of the advent of the routine satellite data, but also a trend in PC2 of the differences.

402 Thus, our overall conclusion is that the global gridded SST datasets correctly describe the  
403 main features of variabilities and trends in regional waters, but that significant improvements  
404 in the regional analyses may be gained when quality controlled homogenized data are  
405 incorporated. In particular for the time prior to the usage of remote sensing by satellites, and  
406 in regions where observational efforts have been limited, such efforts are valuable  
407 contributions to climate variability and change studies. Our example should also be an  
408 encouragement for national climate services to revisit regional data, and to invest into the  
409 elimination of inconsistencies caused by inhomogeneities. There are several projects or  
410 researches dedicated quality control and homogenization of *in situ* data (Kuglitsch et al., 2012;  
411 Hausfather et al., 2016; Minola et al., 2016). It is useful to keep some high-quality data  
412 separate from that available for analyses, for validation activities such as our work and others'  
413 work (Hausfather et al., 2017).



414

415 **Figure 7.** Simulated SSTs at different distances from each coastal hydrological station in the South China  
 416 Sea.



417

418 **Figure 8.** The mean SST differences at the 26 locations between LH and LA-OISST (1982-2015; red  
 419 line), LH and LA-ERSST (1960-2015; blue line), LH and LA-COBE SST (1960-2015; green line) and  
 420 LH and LA-HadISST (1960-2015; black line)

421

422 *Data availability.* All the four gridded SST analyses used in this study are publicly available  
 423 and can be downloaded freely from the websites shown in Table 1. The observational in situ  
 424 SST data from the coastal stations and the coordinates of coastal stations can be obtained from  
 425 the National Marine Science Data Center, National Science & Technology Resource Sharing  
 426 Service Platform of China (<http://mds.nmdis.org.cn>). However, the observational in situ SST

427 data from only 9 coastal stations are publicly available. SST data from the rest stations can be  
428 obtained after an application to the website.

429 *Acknowledgments.* The work is funded by the program of National Natural Science  
430 Foundation of China (No. 41376014; No. 41706020), the National Key Research and  
431 Development Program of China (No.2018YFA0605603; No. 2017YFC1404700) and also  
432 supported by the Hamburg University's Cluster of Excellence CliSAP in Germany,  
433 Shengquan Tang's work is funded by the Chinese Scholarship Council.

434

### 435 **References**

436 Belkin, I. M.: Rapid warming of Large Marine Ecosystems, *Progr Oceanogr*, 81(2009),  
437 207-213, 2009.

438 Belkin, I.M., Lee, M.-A. Long-term variability of sea surface temperature in Taiwan Strait.  
439 *Climatic Change*, 124 (4), 821-834, 2014.

440 Burrow, M. T., et al. The pace of shifting climate in marine and terrestrial ecosystems,  
441 *Science*, 334, 652-655, 2011.

442 Bungel, L. and Clarke, Allan J.: A verified estimation of the El Niño index Niño-3.4 since  
443 1877, *J. Climate*, 22(14), 3979-3992, 2009.

444 Guan, J., Cheung, A., Guo, X. and Li, L. Intensified upwelling over a widened shelf in the  
445 northeastern South China Sea, *J. Geophys. Res.*, 114, 2009.

446 Harris, I., Jones, P. D., Osborn, T.J., and Lister, D.H.: Updated high-resolution grids of  
447 monthly climatic observations- the CRU TS3.10 dataset, *Int. J. Climatol.* 34, 623-642,  
448 2014.

449 Hausfather, Z. and Coauthors: Assessing recent warming using instrumentally  
450 homogeneous sea surface temperature records. *Sci. Adv.*, 3, 31601207, 2017.

451 Hausfather, Z., Cowtan, K. Menne, M. J. and Williams Jr., C. N.: Evaluating the impact of  
452 U.S. Historical Climatology Network homogenization using the U.S. Climate Reference  
453 Network, *Geophys. Res. Lett.*, 43, 1695–1701, 2016.

454 Hickox, R., Belkin, I.M., Cornillon, P., Shan, Z. Climatology and seasonal variability of  
455 ocean fronts in the East China, Yellow and Bohai seas from satellite SST data. *Geophys.*  
456 *Res. Letters*, 27(18), 2945-2948, 2000.

457 Hiraharas, S., Ishii, M., and Fukuda, Y.: Centennial-Scale Sea Surface Temperature  
458 Analysis and Its Uncertainty, *J. Climate*, 27, 57-75, 2014.

459 Honkoop R.J.C., der Meer, J.Van, Beukema, J. J. and Kwast D. Does temperature-  
460 influenced egg production predict the recruitment in the bivalve *Macoma Balthica*? *Mar.*  
461 *Ecol. Prog. Ser.*, 64, 229-235,1998.

462 Huang B., and Coauthors. Extended Reconstructed Sea Surface Temperature version 4  
463 (ERSST v4). Part I: Upgrades and intercomparisons. *J. Climate*, 28,911-930, 2015.

464 Ishii, M., Shouji, A., Sugimoto, S., and Matsumoto, T.: Objective analyses of sea-surface  
465 temperature and marine meteorological variables for the 20th century using ICOADS  
466 and the Kobe Collection, *Int. J. Climatol.*, 25, 865-879, 2005.

467 Jin, Q. H. and Wang, H.: Multi-time scale variations of sea surface temperature in the China  
468 Seas based on the HadISST dataset, *Acta. Oceanol. Sin.*, 30, 14-23, 2011.

469 Kim, K.Y., North, G.R. and Huang, J.P.: EOFs of one dimensional cyclostationary time  
470 series: Computation, examples, and stochastic modeling, *J. Atmos. Sci.*, 53, 1007-1017,  
471 1996.

472 Kuglitsch, F.G., Auchmann, R., Bleisch, R., Bronnimann, S., Martius, O., and Stewart, M.:  
473 Break detection of annual Swiss temperature series. *J. Geophys. Res.*, 117(D13105), 1-  
474 12, 2012.

475 Li, Y., Wang, G.S., Fan, W.J., Liu, K.X., Wang, H., Tinz, B., von Storch, H., and Feng, J. L.:  
476 The homogeneity study of the sea surface temperature data along the coast of the China  
477 Seas, *Acta. Oceanol. Sin.* 40, 17-28, 2018 (in Chinese but with English abstract).

478 Li, Y., Mu, Lin, Liu, Y. L., Wang, G.S., Zhang, D.S., Li, H., Han, X. Analysis of variability  
479 and long-term trends of sea surface temperature over the China Seas derived from a  
480 newly merged regional data set. *Climate Research*, 73, 217-231, 2017.

481 Lima, F.P. and Wethey, D.S. Three decades of high-resolution coastal sea surface  
482 temperatures reveal more than warming, *Nat. Commun.*, 3,704, 2012.

483 Liu, Q.Y. and Zhang, Q.: Analysis on long-term change of sea surface temperature in the  
484 China Seas, *J. Ocean University China* 12, 295-300, 2013.

485 Mantua, N.J. and Hare, S.R.: The Pacific decadal oscillation, *J. Oceanogr.*, 58, 35-44, 2002.

486 Minola, L., Azorin-Molina, C., and Chen, D. L.: Homogenization and assessment of  
487 observed near-surface wind speed trends across Sweden, 1956-2013. *J. Clim.*, 29(20),  
488 7397-7415, 2016.

489 Rayner, N.A., Parker, D.E., Horton, E.B., and others: Global analyses of sea surface  
490 temperature, sea ice, and night marine air temperature since the late nineteenth century,  
491 *J. Geophys. Res.*, 108(D14),1063-1082, 2003.

492 Reynolds, R.W., Smith, T.M., Liu, C.Y., Chelton, D.B., Casey, K.S. and Schlax, M.: Daily  
493 high-resolution-blended analyses for sea surface temperature, *J. Climate*, 20, 5473-5496,  
494 2007.

495 Park, K. A., Lee, E.Y., Chang, E., and Hong, S.: Spatial and temporal variability of sea  
496 surface temperature and warming trends in the Yellow Sea. *J. Mar. Sys.* 143, 24-38,  
497 2015.

498 Saji, N. H., Goswami, B. N., Vinayachandran, P.N., Yamagata, T.: A dipole mode in the  
499 tropical Indian Ocean, *Nature* 401, 360-363, 1999.

500 Sen, P.K.: Estimates of regression coefficient based on Kendall's tau, *J. Am. Stat. Assoc.* 63,  
501 1379-1389, 1968

502 Smith, T.M., Reynolds, R.W., Peterson, T.C. and Lawrimore, J.: Improvements to NOAA's  
503 historical merged land-ocean surface temperature analysis (1880-2006), *J. Climate*,  
504 21(10), 2283-2296, 2008.

505 Su, J., Xu, M., Pohlmann, T., Xu D., Wang D. A western boundary upwelling system  
506 response to recent climate variation (1960–2006), *Cont. Shelf Res.*, 57(2013)3-9, 2012.

507 Tang, S., von Storch, H. Chen, X., and Zhang, M. "Noise" in climatologically driven ocean  
508 models with different grid resolution, *Oceanologia*, 10.1016/j.oceano.2019.01.001,  
509 2019.

510 Tokinaga, H., Xie, S.P., Deser, C., Kosaka, Y. and Okumura, Y. M.: Slowdown of the  
511 Walker circulation driven by tropical Indo-Pacific warming, *Nature*, 491(7424), 439-43,  
512 2012.

513 Vecchiga, Clement, A., Soden, B.J.: Examining the Tropical Pacific's Response to Global  
514 Warming, *Eos Transactions American Geophys Union*, 89(9), 81–83, 2008.

515 Von Storch, H. and Zwiers, F.W.: *Statistical analysis in climate research*. Cambridge  
516 University Press: London, 1999.

517 Wang, Q.Y., Li, Y., Li, Q.Q., et al. A comparison and evaluation of two centennial-scale sea  
518 surface temperature datasets in the China Seas and their adjacent sea areas, *J. Trop.*  
519 *Meteor.*, 24(4), 452-460, 2018.

520 Wernberg, T., Bennett, S., Babcock, R.C., et al. Climate-driven regime shift of a  
521 temperature marine ecosystem, *Science*, 353, 169–172, 2016.

522 Wu, L. X., Cai, W. J., Zhang, L.P., and others: Enhanced warming over the global  
523 subtropical west boundary currents, *Nat. Clim. Change*, 2(3), 161-166, 2012.

524 Xie, S.P., Xie, Q., Wang, D., and Liu, W.T. Summer upwelling in the South China Sea and  
525 its role in regional climate variations, *J. Geophys. Res.*, 108(C8), 3261,  
526 doi:10.1029/2003JC001867, 2003.

527 Xie, S.P., Clara, D., Gabriel, A. V., Ma, J., Teng, H.Y. and Andrew, T. W.: Global warming  
528 pattern formation: sea surface temperature and rainfall, *J. Climate*, 23(4), 966-986,  
529 2010.

530 Xu, W.H., Li, Q.X., Wang, X.L., Yang, S., Cao, L.J. and Feng, Y.: Homogenization of  
531 Chinese daily surface air temperature and analysis of trends in the extreme temperature  
532 indices, *J. Geophys. Res.*, 118(17), 9708-9720, 2013.

533 Yan, T.Z. A preliminary classification of coastal upwellings in the China Seas. *Mar. Sci.*  
534 *Bull.*, 10(6), 1-6, 1991. (in Chinese with English abstract)

535 Yeh, S.W. and Kim, C. H.: Recent warming in the Yellow/East China Sea during winter and  
536 the associated atmospheric circulation, *Cont. Shelf Res.*, 30, 1428-1434, 2010.

537 Zhao, B.R., Ren, G.F., Cao, D.M., Yang, Y.L. Characteristics of the ecological environment  
538 in upwelling area adjacent to the Changjing River Estuary, *Oceanol. Limnol. Sin.*, 32(3),  
539 327-333, 2001. (in Chinese with English abstract)

540



541 **Appendix A: Consistency of homogenized SST data set with homogenized SAT data set**

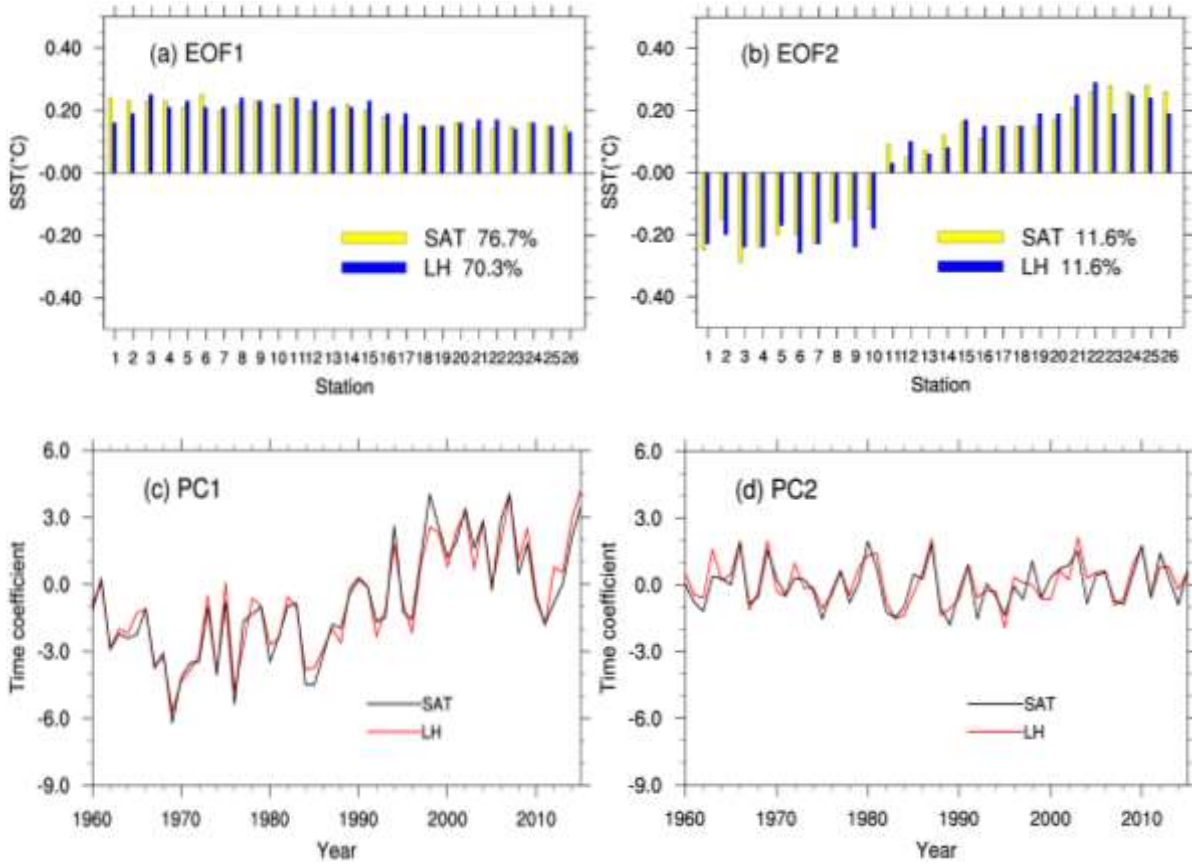
542 We examine if the SST data is consistent with other local homogenized data, specifically with  
543 time series of surface air temperature (SAT) at various locations along the Chinese coast. This  
544 data set contains data from many sites. For each of the SST measuring sites, there is at least  
545 one SAT stations within 100 km distance. We form 26 pairs of located SST/SAT data. SST  
546 and SAT data directly are not compares pairwise, but in terms of the patterns and coefficient  
547 time series (PCs) of their empirical orthogonal functions (EOFs).

548 The first EOFs of SST and *in situ* SAT describe an overall warming, with a slight tendency of  
549 stronger warming in terms of both SST and SAT in the northerly Bohai and Yellow Sea (Fig.  
550 A1a). This pattern is dominant, representing 70.3% and 76.7% of the total interannual  
551 variance. The warming is mostly continuous from about 1970 until 2010 (Fig. A1c). The  
552 similarity of the principal components – expressed by 0.97 in terms of the correlation  
553 coefficient – is striking (Fig. A1c). The second EOFs represent considerably less variance –  
554 namely about 11.6% (Fig. A1b). They describe a North-South contrast, and stationary PCs,  
555 varying around 0 without prolonged positive or negative excursions (Fig. A1d). Also the PCs  
556 of the second PCs of SST and SAT show a remarkably parallel development – with a high  
557 correlation of 0.86 (Figs.A1d).

558 When this exercise is repeated with CRU TS 3.24.01 instead of the *in situ* SAT series, we find  
559 similar consistency (see Fig. SOM-1). The PCs of SAT-CRU also show high correlations of  
560 0.94 and 0.83 with the *in situ* SST (see Fig. SOM-1).

561 We conclude that the two data sets are consistent; the first EOFs describe the warming of the  
562 recent decades of years; the second EOFs describe interannual variability, and may be  
563 influenced by ENSO and other patterns of natural variability. We furthermore conclude that  
564 the new description of SST variability and trends at the 26 sites along the Chinese coast  
565 presents a reliable account of the past since 1960 – and thus may serve as a benchmark for  
566 assessing global analyses of SST datasets.

567



568

569

570 **Fig. A1.** Comparison of the EOF1 and EOF2 derived from the LH data set of local SST at 26 sites (blue  
 571 bars; red lines), and derived from the SAT at the same sites (yellow bars; black lines).  
 572 Top: EOF spatial patterns, bottom: principal components (time coefficients).

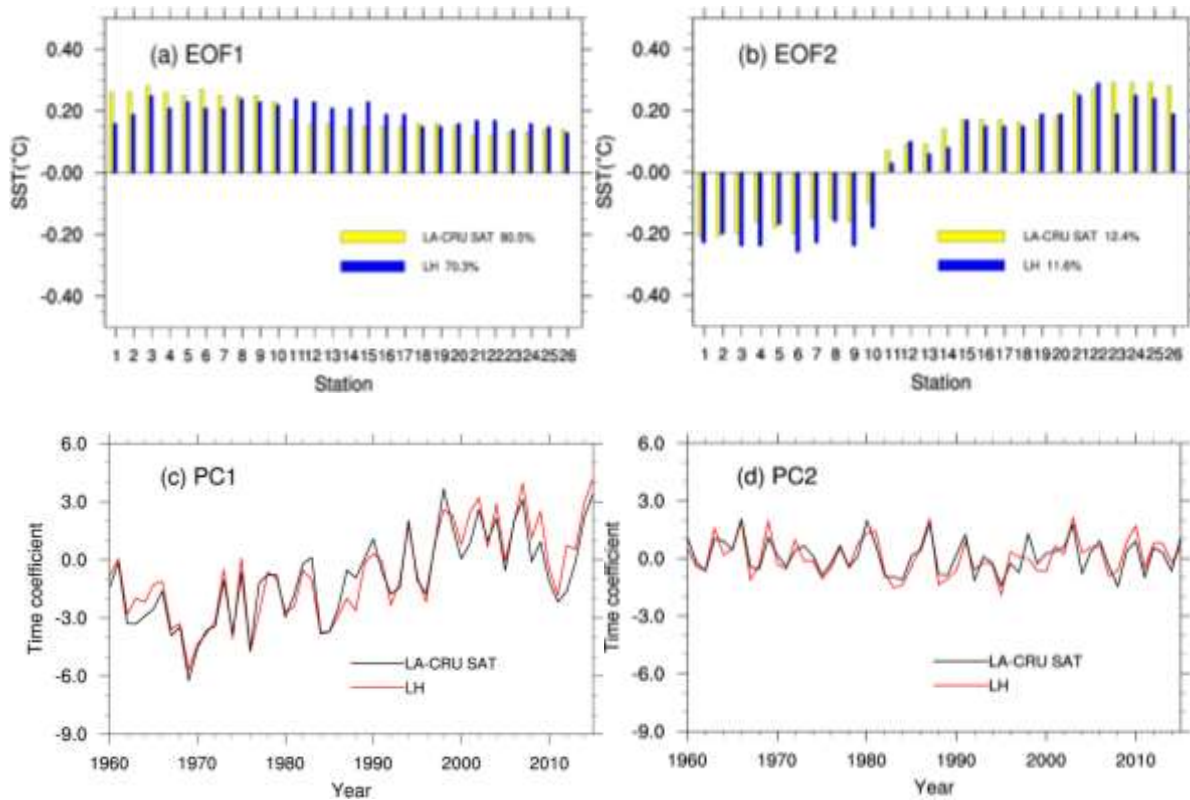
573

574

575

## Appendix B: Supplementary Online Material (SOM)

576



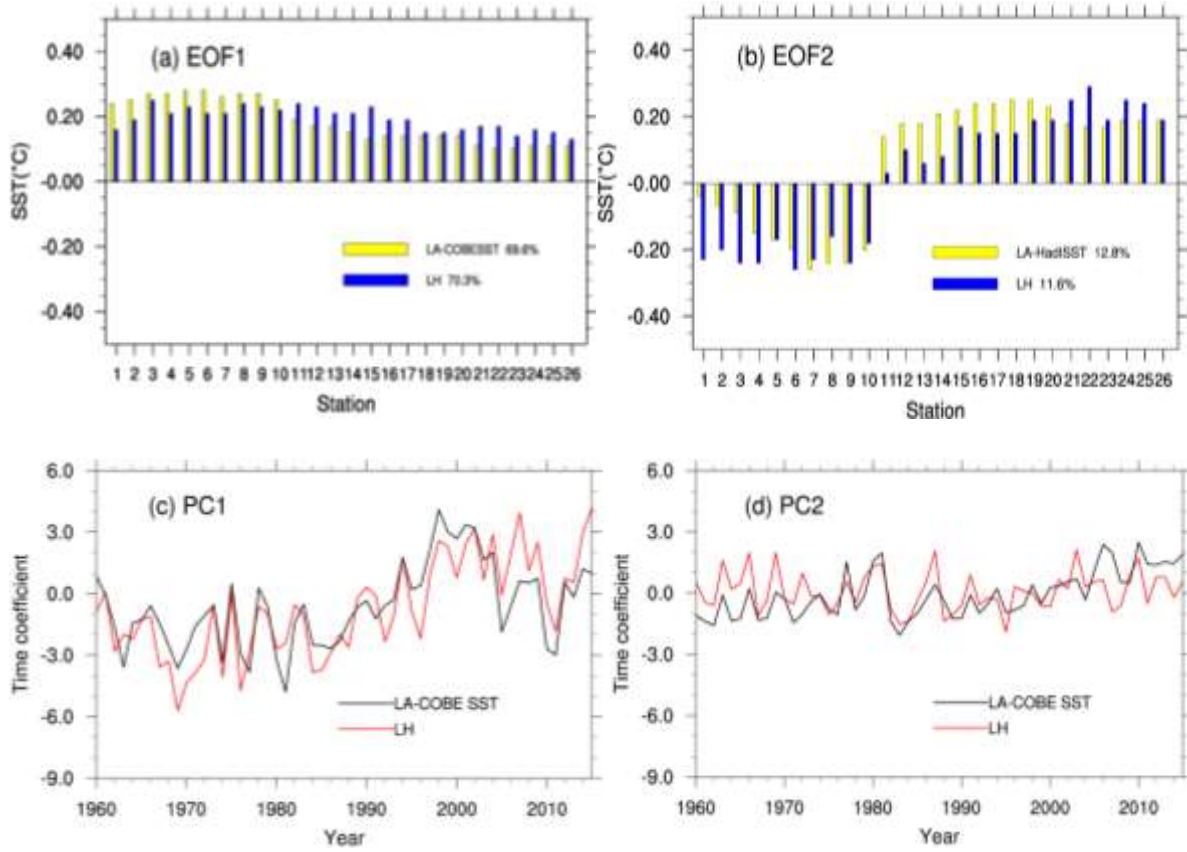
577

578

579 **Fig. SOM-1.** Comparison of the EOF1 and EOF2 derived from the LH data set of local SST at 26 sites  
580 (blue bars; red lines), and derived from the CRU SAT at the same sites (yellow bars; black lines).

581 Top: EOF spatial patterns, bottom: principal components (time coefficients).

582

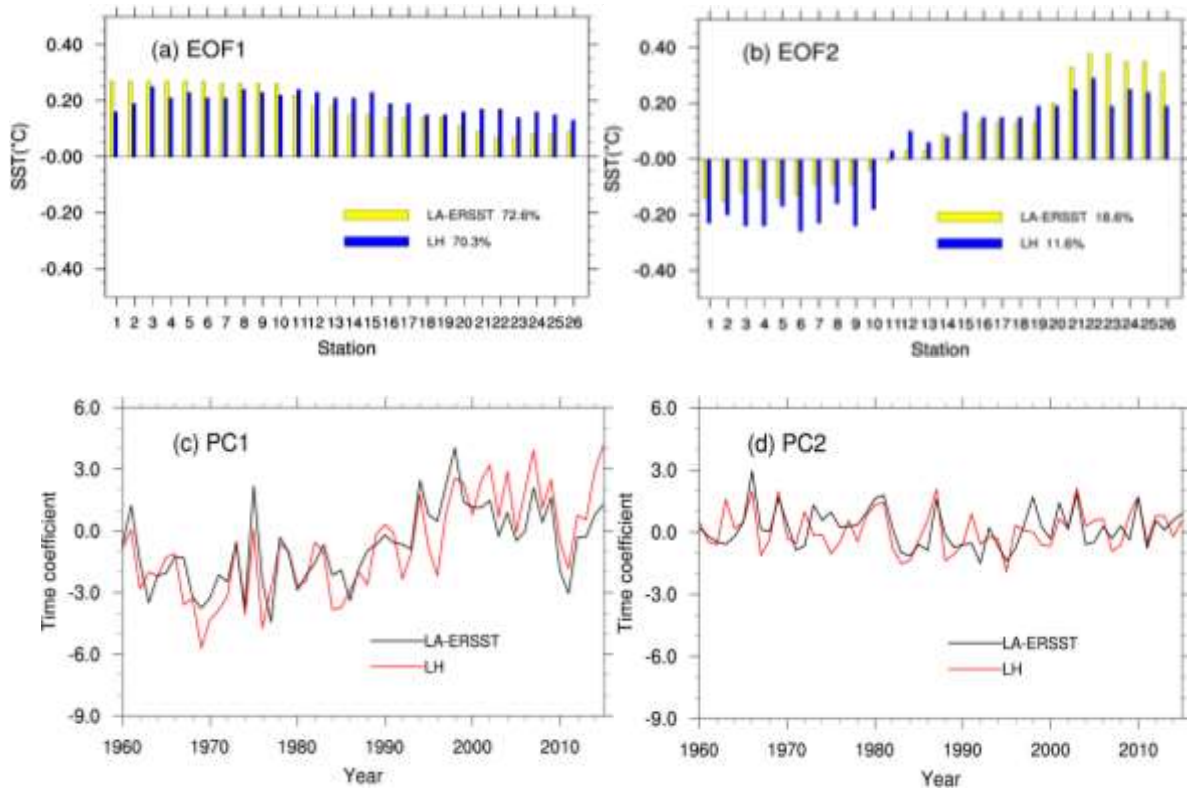


583

584

585 **Fig. SOM-2.** Comparison of the EOF1 and EOF2 derived from the LH data set of local SST at 26 sites  
 586 (blue bars; red lines), and derived from the localized analysis data LA-COBE SST (yellow bars; black  
 587 lines). Top: EOF spatial patterns, bottom: principal components (time coefficients).

588



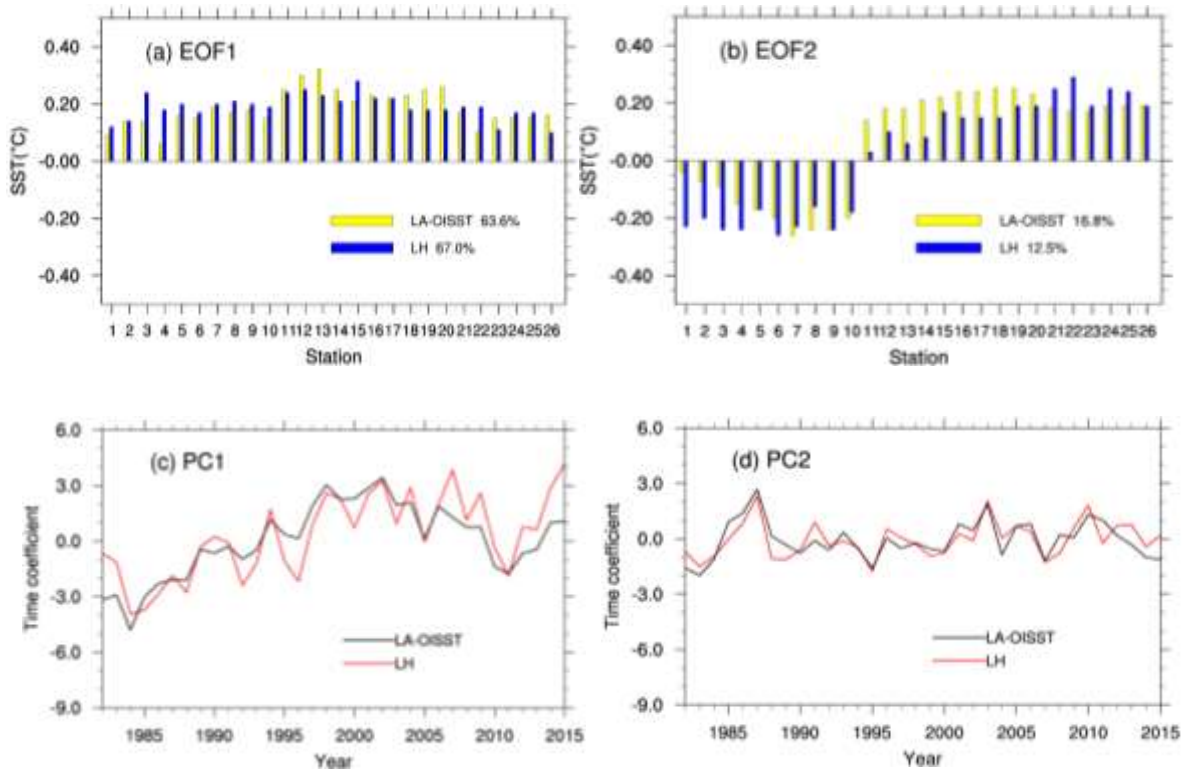
589

590

591

592 **Fig. SOM-3.** Comparison of the EOF1 and EOF2 derived from the LH data set of local SST at 26 sites  
 593 (blue bars; red lines), and derived from the localized analysis data LA-ERSST (yellow bars; black lines).  
 594 Top: EOF spatial patterns, bottom: principal components (time coefficients).

595



596

597

598 **Fig. SOM-4.** Comparison of the EOF1 and EOF2 derived from the LH data set of local SST at 26 sites  
 599 (blue bars; red lines), and derived from the localized analysis data LA-OISST (yellow bars; black lines).  
 600 Top: EOF spatial patterns, bottom: principal components (time coefficients).

601

602 Table SOM-1. Statistics of the time series of the localized SST-analysis (LA-COBE SST) data series at the  
603 26 station, as well as the differences (Diff) between the pairs of time series. The correlation coefficients  
604 between LH and LA-COBE SST are also calculated (the 90% confidence level is 0.22, without considering  
605 serial correlation). Red numbers indicate that the correlation coefficients do not exceed the 90% confidence  
606 level.

No	Mean LA-COBE SST	Diff	Std-dev LA-COBE SST	Diff	Trend ( °C/10yrs)	Diff	Corr
1	11.13	0.38	0.52	0.01	0.17	0.00	0.60
2	11.99	0.22	0.54	0.04	0.16	0.10	0.56
3	12.23	-0.69	0.56	0.14	0.14	0.15	0.74
4	12.70	-1.34	0.59	0.00	0.10	0.11	0.59
5	12.75	0.61	0.60	-0.01	0.10	0.12	0.64
6	12.98	-0.33	0.61	-0.03	0.07	0.10	0.66
7	13.98	-1.89	0.61	-0.02	0.01	0.13	0.68
8	13.83	0.54	0.62	0.03	0.04	0.13	0.72
9	13.83	-0.07	0.62	0.01	0.03	0.19	0.55
10	15.14	-0.29	0.57	0.00	0.03	0.18	0.55
11	19.09	-1.68	0.45	0.20	0.18	0.08	0.77
12	20.94	-3.27	0.43	0.22	0.19	0.05	0.81
13	20.94	-2.74	0.43	0.13	0.19	-0.02	0.78
14	23.25	-3.53	0.38	0.22	0.20	0.01	0.82
15	23.29	-3.30	0.41	0.11	0.20	-0.01	0.79
16	23.29	-1.75	0.41	0.10	0.20	-0.03	0.85
17	22.90	-3.69	0.40	0.14	0.19	0.00	0.78
18	23.33	-2.49	0.41	0.04	0.21	-0.08	0.68
19	23.33	-2.31	0.41	0.02	0.21	-0.08	0.77
20	24.49	-2.06	0.40	0.04	0.18	-0.03	0.81
21	24.95	-1.34	0.33	0.17	0.11	0.07	0.80
22	24.53	-0.93	0.34	0.21	0.10	0.08	0.78
23	24.53	1.26	0.34	0.09	0.10	0.07	0.73
24	25.34	-0.88	0.35	0.14	0.12	0.04	0.77
25	25.34	-0.34	0.35	0.13	0.12	0.04	0.85
26	26.25	-0.45	0.36	0.08	0.13	0.05	0.68

607

608 Table SOM-2 Statistics of the time series of the localized SST-analysis (LA-ERSST) data series at the 26  
609 station, as well as the differences (Diff) between the pairs of time series. The correlation coefficients  
610 between LH and LA-ERISST are also calculated (the 90% confidence level is 0.22, without considering  
611 serial correlation). Red numbers indicate that the correlation coefficients do not exceed the 90% confidence  
612 level.

No	Mean LA-ERSST	Diff	Std-dev LA-ERSST	Diff	Trend ( °C/10yrs)	Diff	Corr
1	12.26	-0.76	0.53	0.00	0.16	0.01	0.69
2	12.06	0.15	0.55	0.03	0.17	0.09	0.70
3	12.68	-1.14	0.54	0.17	0.17	0.12	0.82
4	13.59	-2.23	0.52	0.07	0.16	0.05	0.78
5	12.65	0.71	0.54	0.05	0.16	0.06	0.77
6	13.16	-0.51	0.52	0.06	0.16	0.01	0.79
7	14.62	-2.53	0.50	0.09	0.14	0.00	0.76
8	14.62	-0.25	0.50	0.14	0.14	0.03	0.85
9	14.62	-0.86	0.50	0.12	0.14	0.08	0.78
10	15.92	-1.06	0.50	0.07	0.12	0.09	0.81
11	18.68	-1.27	0.46	0.19	0.10	0.16	0.65
12	21.18	-3.51	0.37	0.28	0.12	0.12	0.70
13	21.18	-2.98	0.37	0.19	0.12	0.05	0.71
14	24.37	-4.39	0.32	0.20	0.12	0.09	0.69
15	24.37	-2.83	0.32	0.19	0.11	0.08	0.75
16	23.02	-3.80	0.33	0.22	0.11	0.06	0.77
17	23.02	-3.30	0.33	0.28	0.12	0.07	0.71
18	24.37	-3.53	0.32	0.13	0.11	0.02	0.63
19	24.37	-3.35	0.32	0.12	0.11	0.02	0.65
20	25.44	-3.01	0.31	0.13	0.09	0.06	0.67
21	25.28	-1.66	0.35	0.14	0.04	0.14	0.56
22	25.23	-1.63	0.41	0.15	0.02	0.18	0.49
23	25.23	0.56	0.41	0.03	0.03	0.17	0.37
24	25.81	-1.35	0.37	0.12	0.01	0.16	0.54
25	25.81	-0.81	0.37	0.11	0.01	0.16	0.66
26	25.96	-0.16	0.34	0.10	0.05	0.13	0.47

613

614